DANMARKS OG GRØNLANDS GEOLOGISKE UNDERSØGELSE **RAPPORT 2020/54**

Preliminary results of CO2-flooding experiment Exp-1

Greensand Phase 1 WP2

Dan Olsen, Samira Mohammadkhani, Rikke Weibel & Niels H. Schovsbo

GEOLOGICAL SURVEY OF DENMARK AND GREENLAND
DANISH MINISTRY OF CLIMATE, ENERGY AND UTILITIES

G E U S

DANMARKS OG GRØNLANDS GEOLOGISKE UNDERSØGELSE **RAPPORT 2020/54**

Preliminary results of CO2-flooding experiment Exp-1

Greensand Phase 1 WP2

Dan Olsen, Samira Mohammadkhani, Rikke Weibel & Niels H. Schovsbo

Confidential report

Copy No.

Released 31.12.2023

GEOLOGICAL SURVEY OF DENMARK AND GREENLAND
DANISH MINISTRY OF CLIMATE, ENERGY AND UTILITIES

G E U S

Table of Contents

Summary and main conclusions

As part of the project Greensand, a CO_2-flooding experiment, Exp-1, was conducted on samples from the Nini-4 well at reservoir conditions (60 ºC, 200 bara). The experiment consists of a complex sequence of CO_2 and formation brine injection operations aimed at investigating possible reactions between supercritical CO_2, formation brine, and the greensand reservoir rock.

The brine permeability measurements agree with the gas permeability determinations of the core samples and gives some information of the brine-CO_2 relative permeability relationship.

The measured permeability to CO_2 is generally lower than the permeability to brine. A sharp drop in permeability was recorded in the third CO_2 flooding operation, which is interpreted as blockage by fines at the outflow end of the core sample. Reversing the flow directions removed the blockage. Apart from this, no permeability anomalies were recorded.

Preliminary investigation of the core sample after the experiment does not reveal significant changes to the greensand rock.

In future project Greensand CO_2-flooding experiments, attempts will be made to avoid blocking by fines at the ends of the core sample.

The experimental flow experiment presented here, together with experiments conducted during “Phase 0”, test the mechanical stability of the reservoir. Together with geochemical stability tests obtained during prolonged exposure of reservoir rocks to CO_2 saturated brine, they aim at documenting the reservoir compatibility to CO_2.

1. Introduction

This report presents the results from the first CO_2 injection experiment of EUDP Greensand Project Phase 1 WP2. The experiment, identified as Exp-1, is the first of a planned series of CO_2 injection experiments intended for evaluating the injectivity of CO_2 into the greensand lithology of the Nini West oil field of Danish North Sea.

The work reported in the present report is preliminary in nature as several aspects of the reported experiment are yet not fully clarified. Therefore, the report is a status report. Previous introductory experiments were presented during "Phase 0" of the project Greensand (Olsen et al. 2020).

2. Materials and experimental method

2.1. Core samples

Sample material was selected from a collection of 1.5" plug samples available from GEUS Core Storage Facility. The samples were originally cut and cleaned by Robertson Research International Ltd. (RRI) as part of a conventional core analysis program reported in MacDonald & Mair (2003). Conventional porosity and permeability analyses are given in MacDonald & Mair (2003). As part of the RRI analytical program the core samples were first Soxhlet cleaned with an azeotropic mixture of chloroform, methanol, and methylamine, then Soxhlet cleaned with toluene, and finally Soxhlet cleaned with methanol.

The RRI samples were in a fair preservation state with apparently reliable core analysis result. Because of this, to save time, and to preserve the limited full core material, it was decided to use the available RRI samples instead of cutting new plug samples.

The samples were in a loosely consolidated state, with sand grains being lost from the samples every time they were handled. Therefore, sample handling was reduced to a minimum.

The cleaning state for the samples was checked by a short Soxhlet cleaning with methanol, where no chloride ions were found. Further cleaning was not conducted. Porosity and permeability analyses were not conducted at GEUS because of the fragile state of the samples.

RRI samples with numbers #90, #91, and #94 were selected for experiment Exp-1 (Fig. 1). Table 1 gives some data for the samples.

Table 1. Exp-1 sample characterization.

Sample Id.			RRI						
	Depth	Orient	Por	Gas perm	Gr. dens.	Diam.	Length	GeomBV	PV
	(MD, m)		(%)	(mD)	(g/ml)	(cm)	(cm)	(ml)	(ml)
90	1774.66	Horiz.	34.0	1160	2.69	3.70	5.01	53.87	18.315
91	1775.04	Horiz.	35.0	1180	2.69	3.70	5.00	53.76	18.816
94	1776.04	Horiz.	35.4	1190	2.70	3.70	5.03	54.08	19.145
Average or mean			34.8	1177	2.69	3.70	15.04	161.71	56.277
Std. dev			0.72	15	0.006	0.00	0.015	0.16	0.418

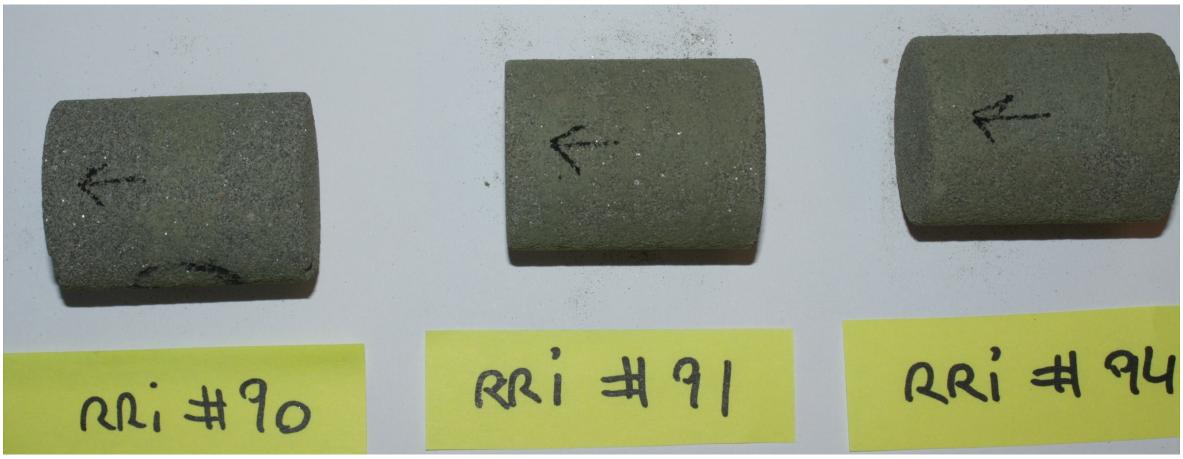

Fig. 1. Plug samples used in experiment Exp-1

2.2. Formation brine

The water used in Greensand Exp-1 is synthetic formation water prepared from the average composition of several water analyses from the greensand reservoirs of the Siri canyon. The average analysis was compiled by Niels Schovsbo (see Olsen et al. (2020). To avoid precipitation of insoluble minerals the contents of Ba^{2+}, HCO_3^-, and Fe_{tot} were reduced in the recipe used for preparing water for Exp-1, cf. Table 2. Also, the contents of Cl^- was adjusted to stoichiometry. This analysis is referred as Nini Formation Water. Water was always degassed by evacuation before being used in experiments.

Table 2. Nini Formation Water used in Project Greensand Exp-1. See Olsen et al. (2020).

Component or Parameter	Mean composition of produced water from Nini (Schovsbo)	Composition used in experiments: Nini Formation Water
Na^+ (mg/l)	29300	29300
Ca^{2+} (mg/l)	4800	4800
Mg^{2+} (mg/l)	1027	1027
K^+ (mg/l)	211	211
Ba^{2+}(mg/l)	123	20
Fe_{tot} (mg/l)	0.9	0.0
Sr^{2+} (mg/l)	602	602
Cl^- (mg/l)	57900	57351
SO_4^{2-} (mg/l)	6.3	6.3
HCO_3^- (mg/l)	100	10
Salinity (wgt%)	n.a.	8.79
Density (g/ml) @ 1 atm, 23 °C (1)	n.a.	1.063
Density (g/ml) @ 200.0 bara, 60 °C (2)	n.a.	1.053
Viscosity (cP) @ 200.0 bara, 60 °C (3)	n.a.	0.565

(1) Fluid density measured at GEUS with Paar DMA 35.
(2) Fluid density measured at GEUS with Paar DMA HPM.
(3) Brine viscosity at reservoir conditions calculated from Kestin et al. (1978)

2.3. Experimental set-up

The three plugs (#90, #91, and #94) were saturated with Nini Formation Water, and were mounted as a composite core sample in a hydrostatic core holder. A steel sieve with 1 mm openings was placed at each end of the composite core sample.

The core holder was mounted in GEUS FC Rig. A particle trap was installed below the vertical core holder, and another particle trap was installed above the core holder. Fig. 2 shows GEUS FC Rig that was used for Exp-1. Please note that in Exp-1 the core holder was in a vertical position, while Fig. 2 shows a horizontal core holder.

Determination of differential pressure is a crucial measurement in reservoir condition experiments with measurement of gas permeability. The low viscosity of supercritical CO_2 necessitates the use of pressure transducers with high precision coupled with high flow rate through the core sample. The pressure transducers used in Exp-1 have a nominal accuracy of 0.10 bar at the conditions of Exp-1. However, the precision (reproducibility) is significantly better, and because the experimental procedure allowed frequent zeroing of the transducers, the differential pressure was determined with a mean error of 0.01 bar. For the CO_2 flooding operations, a flow rate of 800 ml/h (13 ml/min.) was used, which caused successful determination of permeability at differential pressure as low as 0.05 bar.

The experimental conditions for Exp-1 are summarized in Table 3.

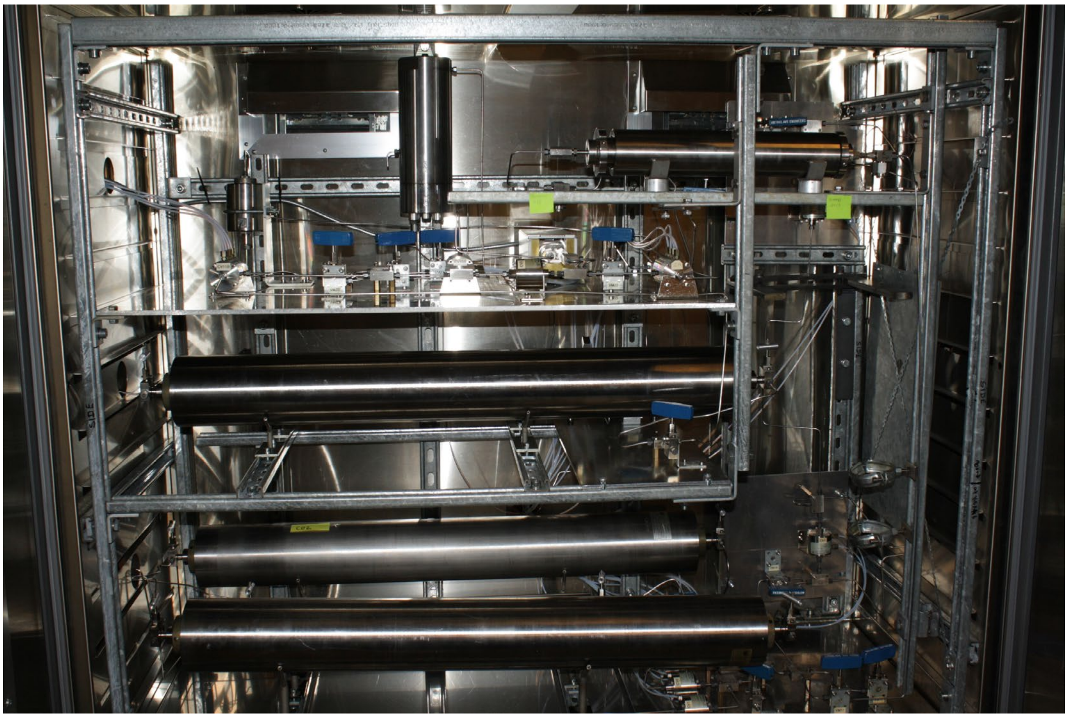

Fig. 2. GEUS FC Rig used for Exp-1, Note that in Exp-1 the core holder was in vertical position.

Table 3. Conditions for Exp-1.

Experiment id.	**Exp-1**
Formation	Frigg Member of Horda Formation
Sample material	Fine-grained glauconitic sand
Sample type	Composite 1.5" plug
Temperature	60 °C
Fluid pressure	200 bara
Hydrostatic confining pressure	220 bara
Net overburden pressure (NOB)	20 bar
Flow direction	Vertical
Formation water	Nini Formation Water
Injection water	Nini Formation Water
Injection CO_2	KVGasteknik purity 4.0

3. Reservoir condition experiments

Summary of operations during core flooding Exp-1:

1. Mounting core holder with 3 greensand samples in GEUS FC Rig
2. Establishing reservoir conditions
3. Measurement of brine permeability @ 800 ml/h
4. CO_2 flooding in upwards direction @ 800 ml/h, 33.5 PV's injected in 2.4 hours
5. Brine flooding in upwards direction @ 100 ml/h, 2.6 PV's injected in 1.5 hours
6. CO_2 flooding in upwards direction @ 800 ml/h, 21 PV's injected in 1.5 hours
7. Brine flooding in upward direction @ 100 ml/h, 0.5 PV's injected in 0.25 hour
8. No-flow condition for 17 hours
9. Brine-flooding in upwards direction @ 100 ml/h, 3.0 PV's injected in 1.6 hour
10. CO_2 flooding in upwards direction @ 800 ml/h, 17.4 PV's injected in 1.2 hours
11. Work to change flow direction
12. CO_2 flooding in downwards direction @ 800 ml/h, 6.0 PV's injected in 0.4 hours
13. Flooding stopped when CO_2 supply ran empty
14. Depressurization and cooling of reservoir rig
15. Dismounting core holder from rig, dismount plug samples from core holder.

3.1. Measurement of brine permeability

Permeability to brine was measured by flooding the core samples with Nini Formation Water at 800 ml/h, cf. Fig. 3. Brine viscosity was calculated to 0.565 cP @ 60 °C, 200 bara, salinity 8.79 wgt% by using equations in Kestin et al. (1978). A brine permeability of 978 mD was measured. The mean value of the 3 gas permeability determinations of RRI is 1177 mD (Table 1). Because brine permeability determinations are usually lower than gas permeability determinations on the same sample (Bloomfield & Williams, 1995), the permeability determinations are considered to agree.

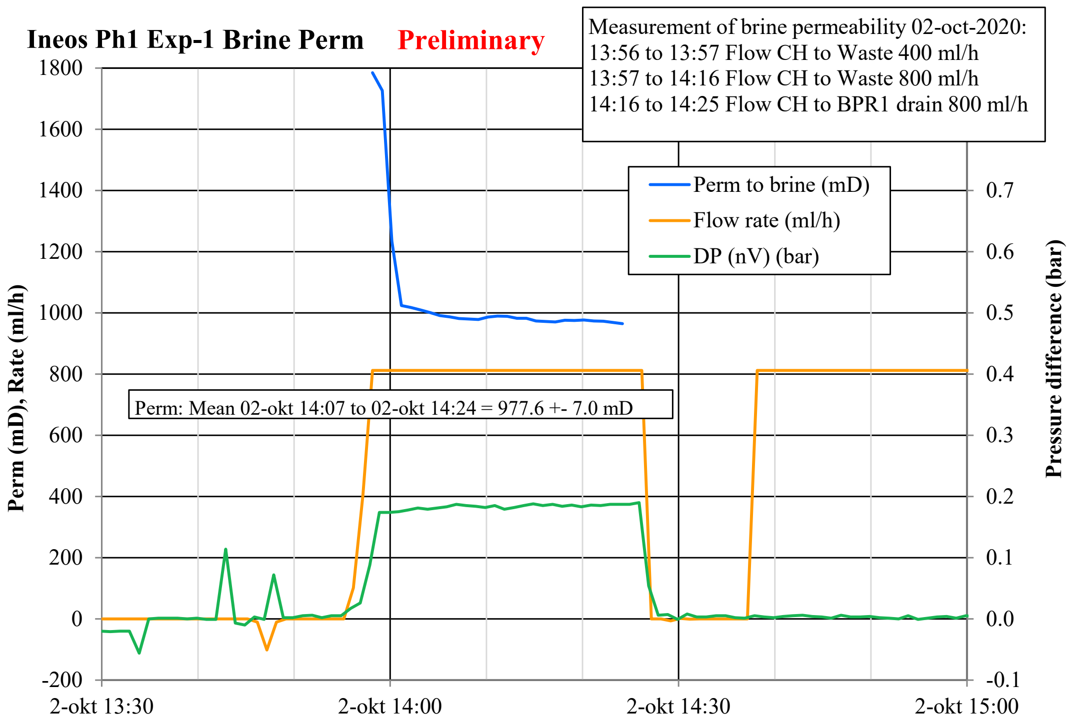

Fig. 3. Experiment Exp-1. Permeability to brine.

3.2. Flooding with CO_2 and brine

Fig. 4 gives an overview of the injection periods of Exp-1. A total of 85.4 pore volumes of fluid (PV's) were injected with alternating injection of CO_2 and Nini Formation Water. The flooding operations covered two days, with a period without flooding during the night between the two days. The period without flooding took place at the end of a short formation water flooding, to allow the core sample to react with formation water saturated with residual CO_2. During the flooding operations the maximum fluid pressure variation was ± 1.2 bar, and the maximum temperature variation was ± 0.09 °C. Therefore, pressure and temperature are considered constant at 200 bara and 60 °C.

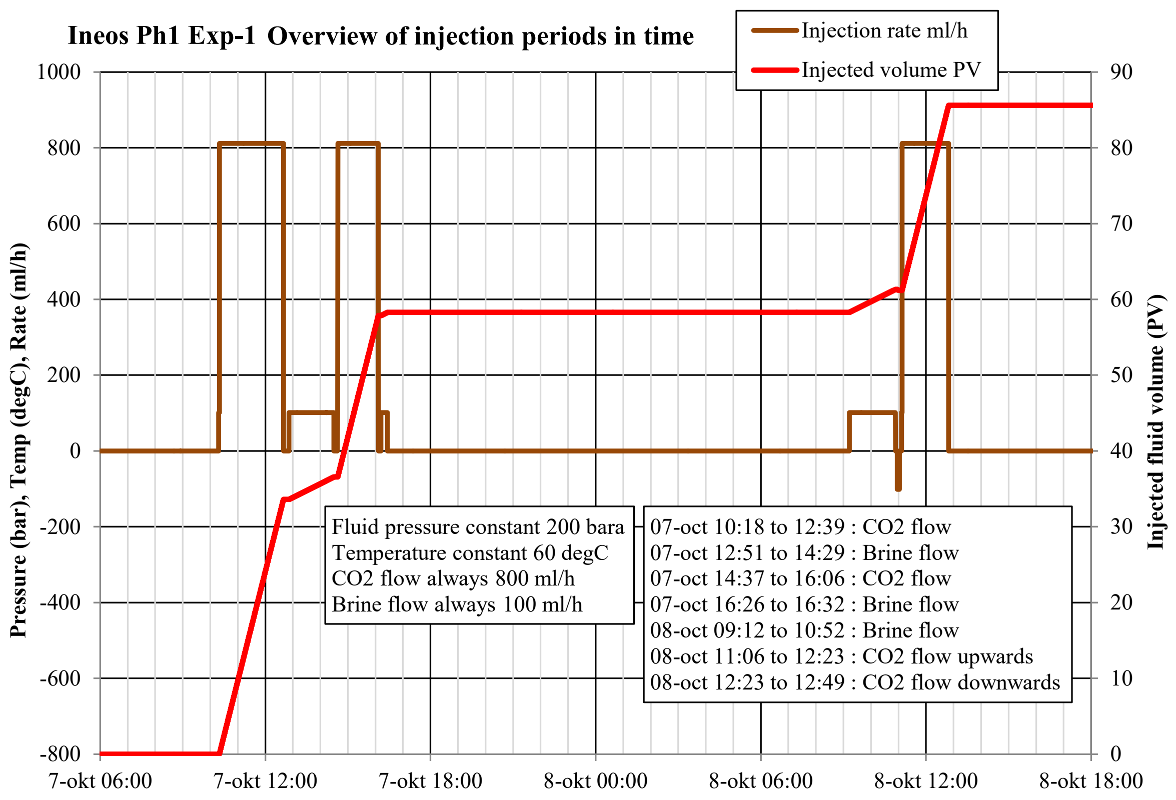

Fig. 4. Experiment Exp-1. Overview of flooding operations.

Fig. 5 shows the flooding operations plotted against injected pore volume. The plot shows three periods with CO_2 injection separated by two periods with brine injection.

Please note that the first period with brine injection contains a short period from PV 36.1 to PV 36.4 without dP data. The missing data occurs towards the end of the brine injection period, but the dP data was restored shortly before the end of the brine injection period, and valid permeability data are seen as a short blue line at PV 36.4 and 450 mD.

Also please note that the second brine injection period contains the break without flow at PV 58.1. When flow was restarted, it took some time before dP came to equilibrium. In the disequilibrium period the calculated permeability is erroneous and therefore the permeability spike at PV 58.1 should be disregarded. The same should applies to all other permeability anomalies associated with flow rate changes.

The two first periods with CO_2 flooding are very similar. At the beginning of each CO_2 flooding period the permeability increases steeply, followed by a slower and slower rise in permeability. The first CO_2 flooding period ends at a stable permeability of 180 mD, while the second permeability period ends at a stable permeability of 200 mD. Both permeability values are much lower than the pure brine permeability of 978 mD (Fig. 3).

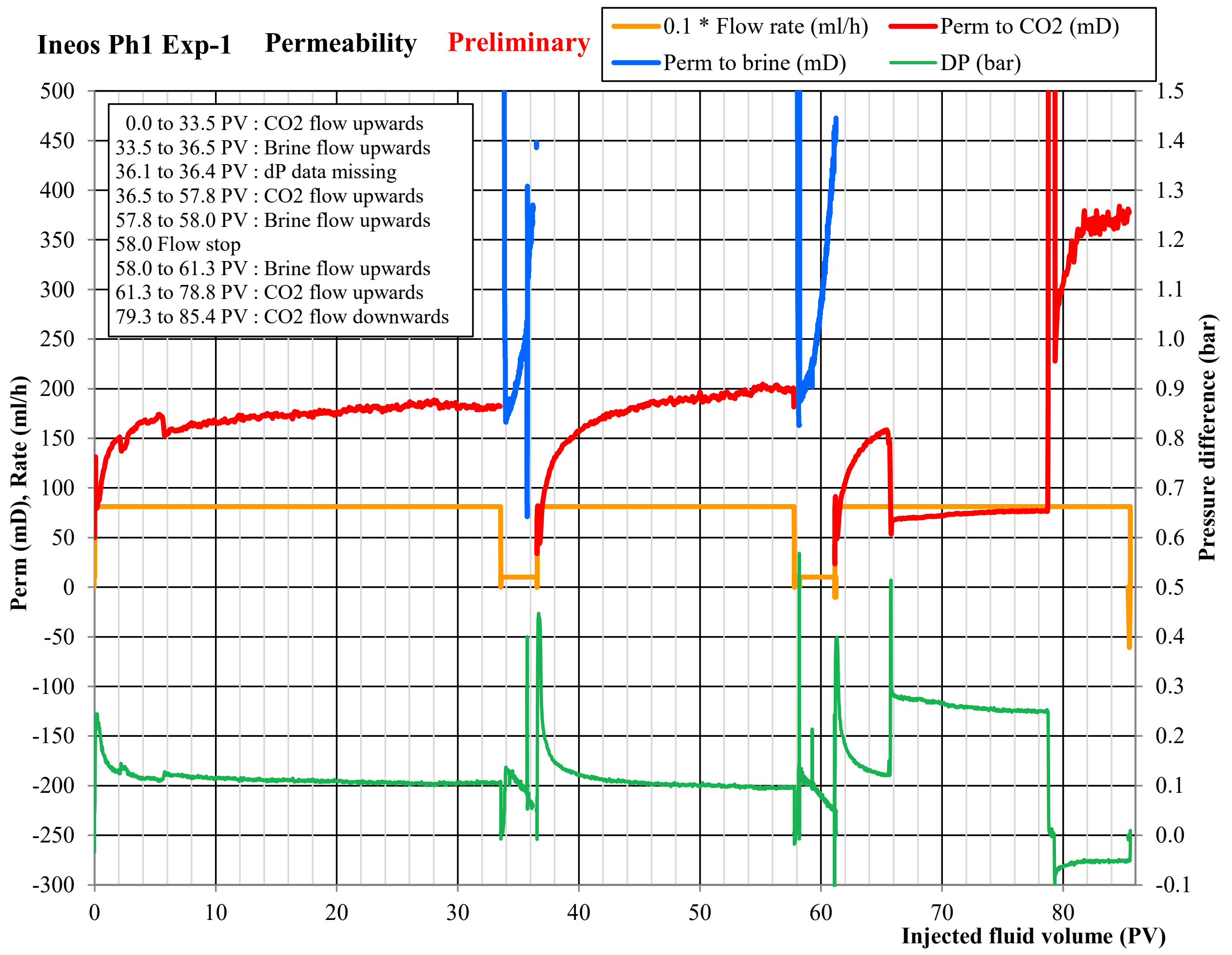

Fig. 5. Experiment Exp-1. Flooding operation.

The two brine injection periods are very similar, showing steep increases in permeability. The permeability curves do not reach stability, however. For both periods, the brine injection reach a brine permeability of approximately 450 mD, but the brine permeability would undoubtedly have increased, if brine injection had been continued. The brine injection periods were limited by the volume of brine in the brine supply cylinder.

The third period with CO_2 injection behaved very different from the first two CO_2 injection periods. Initially, the CO_2 permeability increased like the two first CO_2 injection periods. However, at PV 65.7 a sharp drop in permeability occurred with permeability changing abruptly from 160 mD to approximately 40 mD. The drop in injectivity cannot be related to any external cause. After the drop in permeability, the permeability quickly recovered to 68 mD, and then at a slow rate to 72 mD. The experiment operator observed the development and decided to reverse the flow direction in the core sample. The flow reversal operation took place from PV 78.8 to PV 79.3. During the flow reversal operation, the core sample had no flow. When flow was resumed in reverse direction, the permeability immediately recovered to a permeability level that was higher than in the first two CO_2 injection periods. Furthermore, the permeability continued to increase, and reached 375 mD at the end of the experiment. The CO_2 injection stopped when the CO_2 supply was empty which occurred at PV 85.4 (Fig. 5). At this time the permeability to CO_2 was still slowly rising.

Fig. 6 shows a close-up of the permeability drop that occurred at PV 65.7. The sharp increase in dP takes place in only 0.048 PV, equivalent to injection of 2.8 ml of CO_2. The following quick increase in injectivity took place at the same speed, within 0.048 PV. The logging interval was 6 seconds, equivalent to 0.024 PV at rate 800 ml/h.

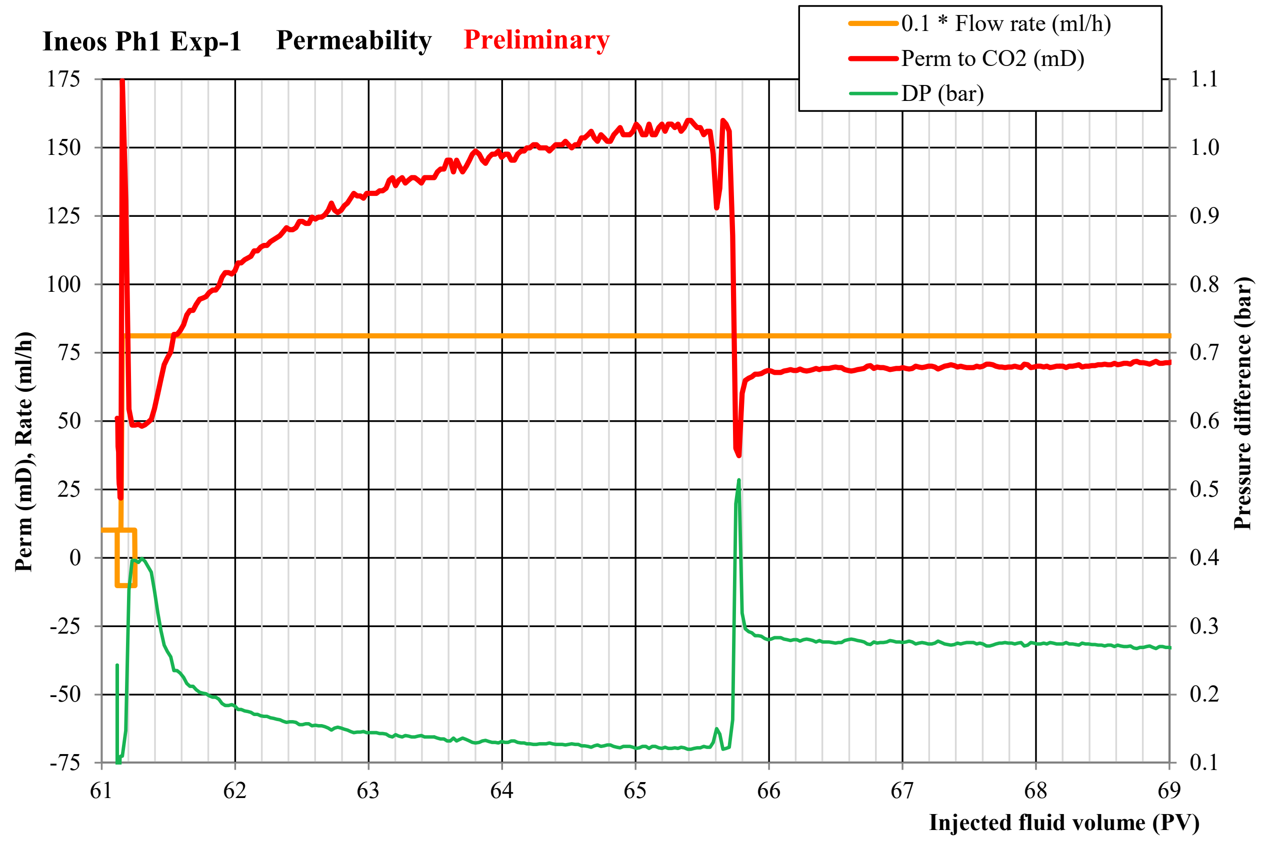

Fig. 6. Experiment Exp-1. Drop in injectivity at PV 65.7.

An incident occurred during the first brine flooding period, where NOB abruptly decreased from 20 to 5 bar, with derived fluctuations in dP cf. Fig. 7. The cause of the incident is not clear. The automatic NOB control program of the reservoir rig quickly restored NOB to the nominal value of 20 bar, but the incident did cause a significant increase in brine permeability. The increasing trend in the brine permeability curve was not disturbed.

A similar drop in NOB was recorded 5 hours later at a time where no flow took place. This time NOB decreased to 6.6 bar, and again recovered by the automatic NOB control program.

The cause of the two incidents of NOB decrease is not clear. The automatic NOB control program has been used for many years and is considered very reliable. In future experiments, attention will be paid to possible causes of NOB decrease incidents.

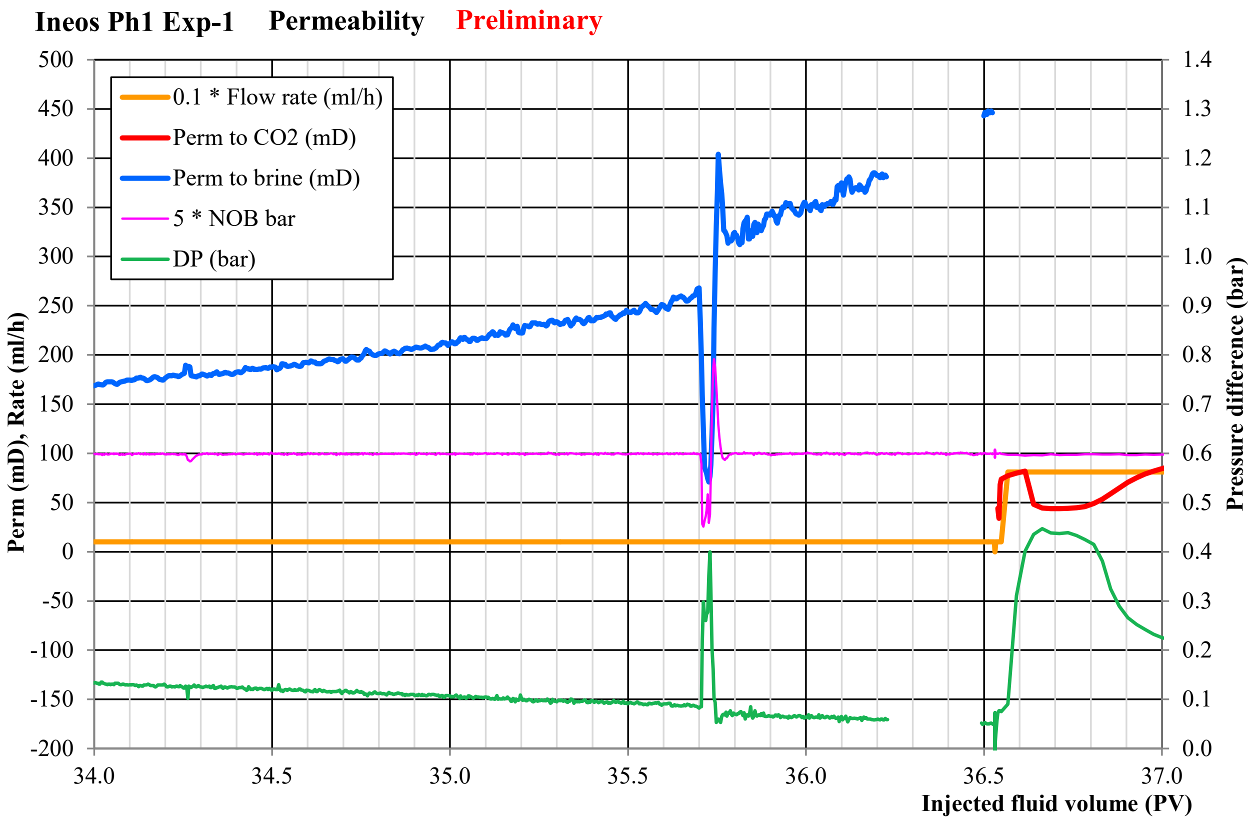

Fig. 7. Experiment Exp-1. Drop in NOB at PV 35.7.

4. Rock mechanical aspects of experiment

During Exp-1 the position of the core holder floating piston was measured 5 times, Fig 8. The measurements were made with a simple electronic caliper, with an estimated uncertainty of 0.04 mm. To make the measurements it was necessary to open the rig oven, and therefore the measurements were only made when the resulting temperature fluctuations did not disturb the flooding operations.

During establishment of reservoir conditions, from September 23rd to 25th, the floating piston retracted approximately 0.1 mm. This is common during establishment of reservoir conditions, and probably mainly reflects settling of the core holder end pieces.

In the period at reservoir conditions before the CO_2-flooding, no significant movement of the core holder piston was seen, as the recorded positions are within measuring uncertainty.

During the CO_2-flooding period, from October 6th to 9th, the core holder piston retracted approximately 0.1 mm, which is considered above the measuring uncertainty. It thus seems that the CO_2- and brine-floodings effected a slight compaction of the core sample, with a length reduction of approximately 0.7%.

After experiment Exp-1 the core samples appeared unaffected by the flooding experiments. The samples are currently being investigated for effects of the flooding experiments on porosity, permeability, and mineralogical changes.

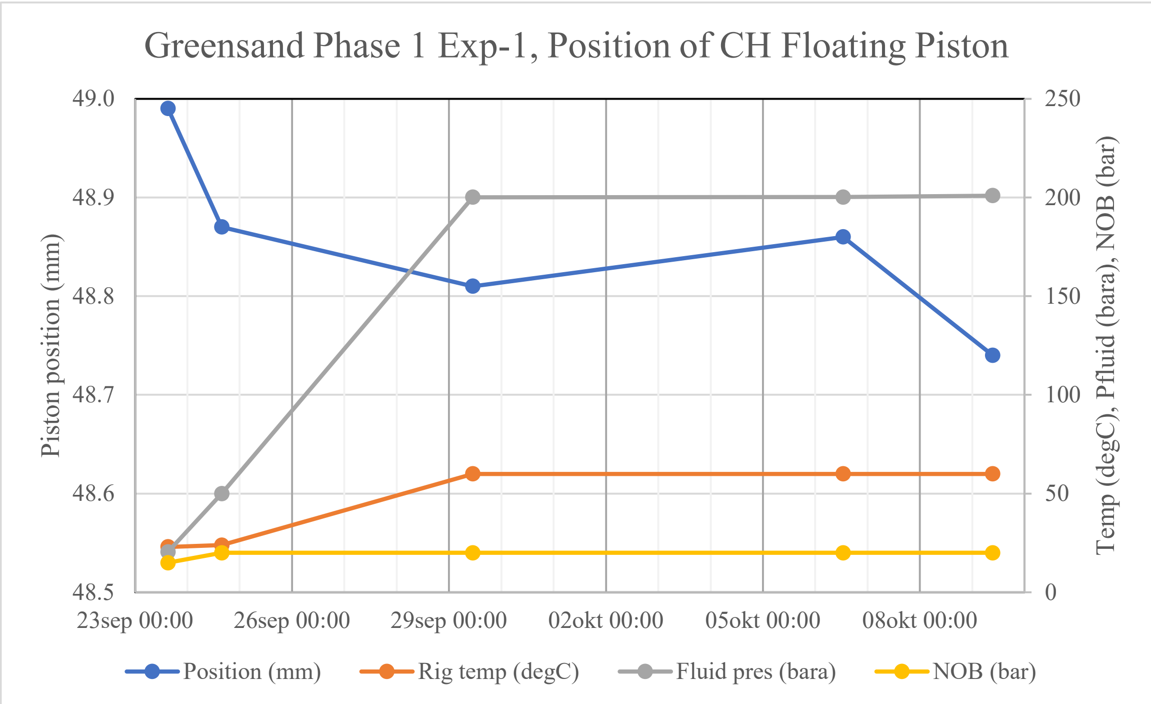

Fig. 8. Experiment Exp-1. Position of core holder floating piston. CO_2 flooding operations took place October 7th to 8th. Estimated uncertainty of measurements is 0.04 mm.

5. Production of fines

At the end of Exp-1, water samples were taken to possibly collect fines and characterize their mineralogy.

1. A sample of water was taken from the Waste Cylinder. No fines were present.
2. The lower particle trap was examined, and a sample of fines was recovered, sample id Fines-1.
3. The upper particle trap was examined, and a sample of fines was recovered, sample id Fines-2.
4. The fixed end piece of the core holder, i.e. the lower end piece, was examined, and a sample of fines was recovered, sample id Fines-3.
5. The floating end piece of the core holder, i.e. the upper end piece, was examined, and a sample of fines was recovered, sample id Fines-4.

The particles of the water samples were concentrated by filtering through a filter with pore sizes 8 µm (Fig. 9). The dried particles were mounted on stubs, coated with platinum and investigated by a Zeiss Sigma 300 VP field emission scanning electron microscope (SEM) at GEUS operating at 15 kV and 40–100 nA and equipped with two Bruker Xflash 6|30 30 mm^2, 129 eV EDS detectors.

The samples from the core holder, both fixed and floating ends, consisted of sand sized grains of quartz, glauconite, K-feldspar and mica (Fig. 10). Fibres were probably an artefact from the filters.

The samples from the traps had a content of sand sized grains of quartz, glauconite, K-feldspar and mica, like the samples from the core holder (Fig. 11). In addition, the lower trap contained metal flakes of iron and chromium, and rare metal fragments of iron, chromium and nickel besides rare phosphorous fragments (Fig. 11). The metal flakes could origin from steel parts in the experimental set up. The sand sized grains in the upper trap had a comparably larger content of mica than the other samples.

It is noteworthy, that the individual sand grains seem to be intact and not disintegrated.

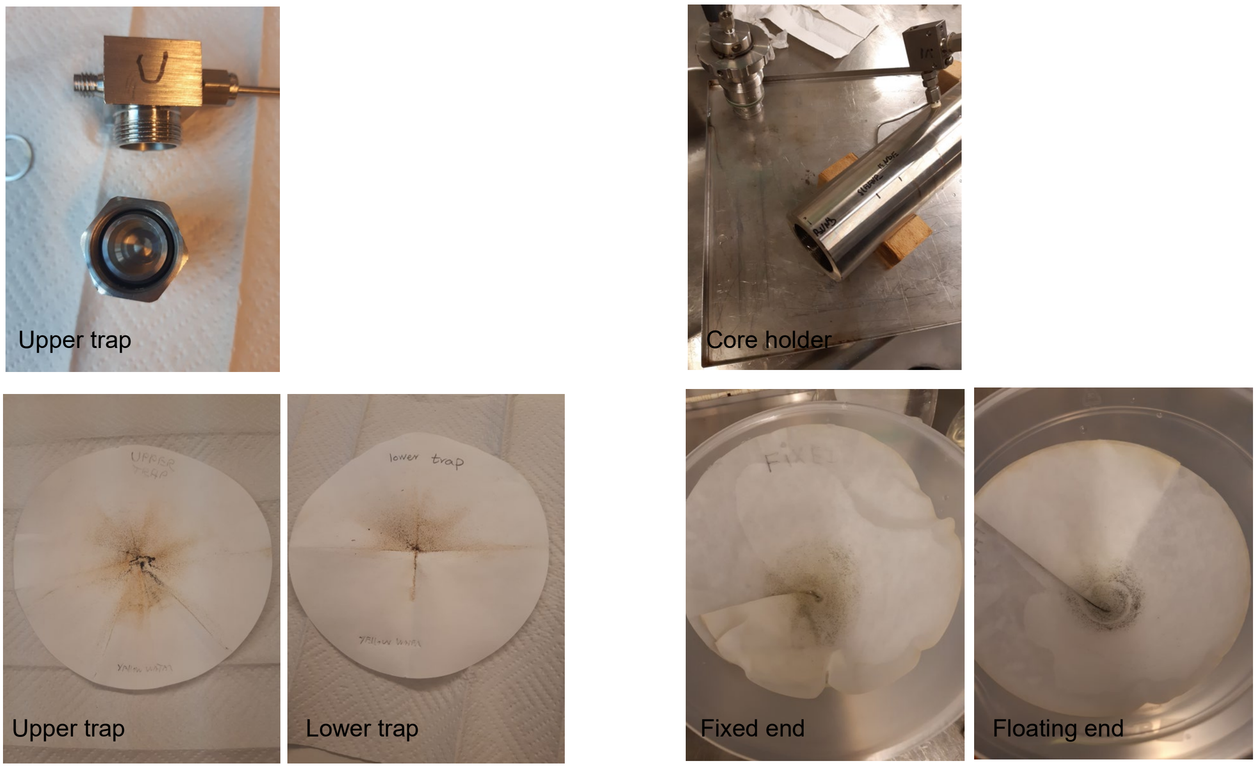

Figure 9: Samples concentrated on filters from upper trap, lower trap, fixed end, and floating end of the core holder.

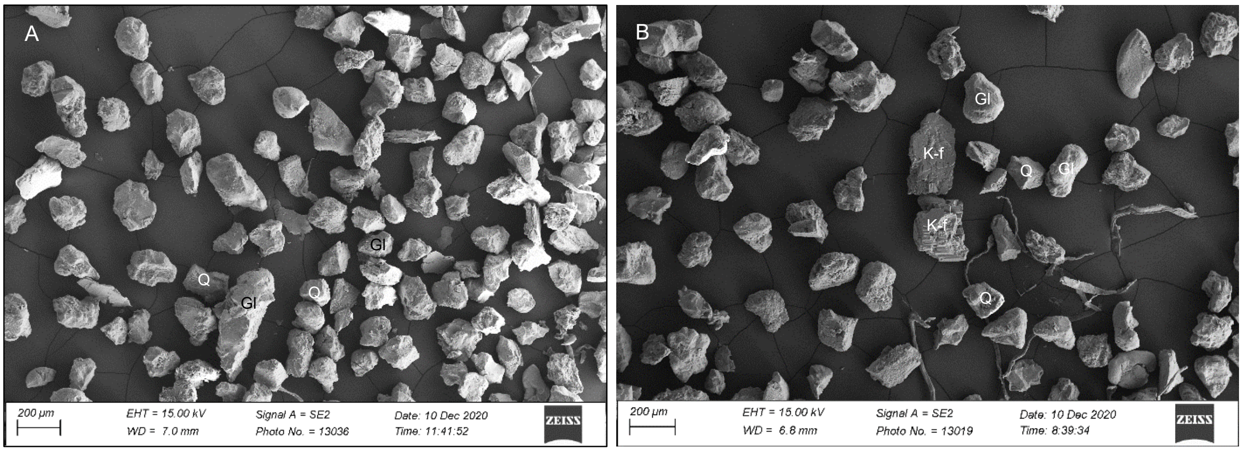

Figure 10: Sand sized grains consisting of quartz (Q), glauconite (Gl) and K-feldspar (K-f) occurring at the fixed (A) and floating (B) ends of the core holder. Note, that all sand grains seem to be intact. Scanning electron micrograph.

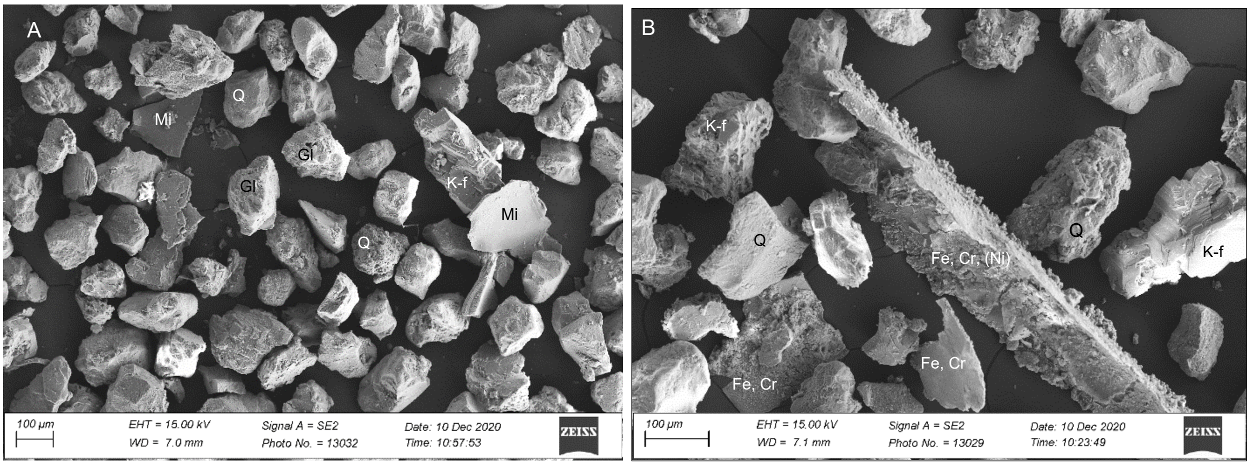

Figure 11: Sand sized grains concentrated on filters from upper (A) and lower (B) traps consist of quartz (q), glauconite (Gl), K-feldspar (K-f) and mica (Mi). Note, metal flakes consisting of Fe, Cr and Ni. Scanning electron micrograph.

6. Discussion

The brine permeability data presented in Fig. 3, with a brine permeability of 978 mD, are stable and in reasonable agreement with the air-permeability of 1177 mD reported by RRI.

A complex flooding scheme was adopted for the CO_2-flooding work with three CO_2-flooding operations separated by two brine-flooding operations. The flooding scheme was completed without serious failures. In general, the GEUS FC Rig worked as expected. The only significant departure from the planned sequence of operations was the two incidents of NOB reduction. These incidents did not seriously affect the experiment, but their cause is not clear. In the future experiments attention will be paid to identify possible causes.

The two brine-flooding operations are very similar as both show that permeability steeply increases from the CO_2-saturated starting point. This is considered an effect of a brine-CO_2 relative permeability system as CO_2

fluid is displaced from the pore space of the core sample by brine flow, and at the same time CO_2 is dissolved into the brine. Both brine-flooding operations ended at a permeability of approximately 450 mD, but at the end of the brine flow, the brine permeability was still steeply increasing. The brine-flooding operations ended because of restricted brine supply. The second brine-flooding operation included a 17 hours period without flow shortly after the beginning of the operation, which did not seem to influence the permeability.

The first two CO_2-flooding operations were very similar, with permeability to CO_2 initially rising steeply from the brine-saturated starting point. After injection of 10–15 pore volumes of CO_2, the permeability rise levelled out at a permeability of 180 to 200 mD. The permeability trend is considered, at least partly, to reflect the brine-CO_2 relative permeability relationship of the core sample, with displacement of brine from the pore space of the core sample, and dissolution of water into CO_2. Precipitation of salt in the pore space may complicate the relationship.

The third CO_2-flooding operation behaved differently. During injection of the first 6 PV's of CO_2 the permeability trend was similar to the first two CO_2-flooding operations, but at 65.7 a sharp drop in permeability occurred (Fig. 6). The drop in permeability took place within only two logging entries, which is 12 seconds equivalent to injection of 2.8 ml of CO_2 or 0.05 PV of CO_2. After the sharp permeability drop, the permeability recovered with the same speed, i.e. within 12 seconds, but only a partial recovery took place to approximately 45% of the permeability before the drop. After that the permeability made slow recovery that was very different from the trend of the first two CO_2-flooding operations.

As it was evident that something was blocking the CO_2 flow, it was decided to reverse the flow direction. The flow reversal was effected at PV 78.8 to 79.3, and had the effect that the CO_2 permeability immediately increased to a high level of 250 to 300 mD, which is significantly higher than the permeability at the end of the two first CO_2-flooding operations. Furthermore, the CO_2 permeability continued to increase to 375 mD. CO_2-flooding stopped when the CO_2-supply was empty, at a time when CO_2 permeability was still slowly increasing.

It is noteworthy that the segment of CO_2 permeability before PV 65.7 and the segment of CO_2 permeability after PV 79.3 approximately follow a common trend (Fig. 5). It could represent a CO_2 permeability trend not seriously affected by fines. Contrary, the CO_2 permeability trend between PV 65.7 and PV 78.8 is considered to represent a trend seriously affected by fines. Fines that move within the pore system of a core sample are considered incapable of causing the fast permeability changes that occurred at PV 65.7 and PV 79. Such fast permeability drop as at PV 65.7 is considered indicative of accumulation of fines against a flow restriction of limited extent. Similarly, the fast permeability increase at PV 79 is considered indicative of the dispersal of a flow blockage.

The most likely position of the flow restriction is at the outlet end of the core holder. Here, the flow through the core sample is confined to enter a hole with 1.8 mm diameter in the end piece of the core holder, and furthermore, the end of the core sample is pressed against the end piece by the hydrostatic construction of the core holder. This seems to enable accumulation of fines at the entrance of the end piece, which could eventually form an aggregate that caused the permeability drop. When the flow direction was reversed, the fines aggregate disintegrated, and the fines were pushed into the steel sieve at the end of the core sample and did not cause further flow blockage.

In the next CO_2 flooding experiment, Exp-2, the construction of the core holder has been modified with particle traps positioned between the core sample and both end pieces of the core holder. The intention is that fines will settle in these particle traps and thus not block the flow. The particle traps are necessarily open to the core sample, and there is a risk that the fragile core sample will disintegrate into the particle traps.

7. Conclusions

A CO_2-flooding experiment was conducted with samples of Nini greensand at reservoir conditions with a complex sequence of CO_2 injection and brine injection operations. The brine permeability measurements agree with the gas permeability determinations of the core samples, and contains information of the brine-CO_2 relative permeability relationship.

Supercritical CO_2 permeability of up to 375 mD was recorded, which is 38% of the brine permeability of 978 mD measured in the present experiment, and 32% of the mean gas permeability measured by RRI on the three core plugs.

A sharp drop in permeability was recorded in the third CO_2 flooding operation, which is interpreted as blockage by fines at the outflow end of the core sample. Reversing the flow directions removed the blockage.

Apart from this no permeability anomalies were recorded.

Preliminary investigation of the core sample after the experiment does not reveal significant changes to the greensand rock

The fines that moved in the experiment are sand sized grains consisting of quartz, glauconite, K-feldspar and mica. The mineralogical composition is identical with a typical glauconitic sandstone from the Nini-4 well. Steel flakes and fibres are most likely artefacts from the experimental setup and the applied filters.

In the next CO_2-flooding experiment, attempts will be made to avoid blocking by fines at the ends of the core sample.

Acknowledgment

The EUDP programme is acknowledged for financial support of Project Greensand. The Project Greensand consists of a consortium of GEUS, INEOS, Maersk Drilling and Wintershall DEA.

References

Bloomfield, J.P., Williams, A.T. 1995. An empirical liquid permeability – gas permeability correlation for use in aquifer properties studies. *Quarterly Journal of Engineering Geology, **28**, S143-S150, 1995.*

Kestin, J., Khalifa, H.E., Abe, Y., Grimes, C.E., Sookiazian, H., Wakeham, W.A. 1978. The effect of pressure on the viscosity of aqueous NaCl solutions in the temperature range 20-150 °C. *J. Chem. Eng. Data **23,4**, 328-336, 1978.*

MacDonald, I., Mair, K. 2003. Nini-4. Conventional core analysis report. Nini-4 (5605/10-1). Licence 4/95. *Robertson Research International Ltd. Report no. AF790, March 2003.*

Olsen, D., Holmslykke, H.D., Weibel, R., Schovsbo, N. 2020. Setup and sample program of CO_2 experiments. Greensand Phase 0. D*anmarks og Grønlands Geologiske Undersøgelser*, report 2020/19.

NIST Chemistry Webbook: National Institute of Standards and Technology, [www.webbook.nist.gov/chemistry. 2020](www.webbook.nist.gov/chemistry).

Danish Ministry of Climate, Energy and Utilities